Bernoulli Vector Anemometer

Hrushikesha Athreya, Mason Camp, Eric Lee

PHYS 371 Design Like a Physicist, Fall 2022

Figure 1: Credit to Kintech Engineering

Contents

1 Abstract

This project is oriented around analyzing the pressure differences recorded from multiple DPS310s which are high-precision pressure sensor modules. Bernoulli's principle describes the inverse relationship between pressure and fluid velocity. Wind, at a low velocity, can be approximated as to be an incompressible fluid. To test Bernoulli's principle, we use multiple DPS310 sensors inside cross-sectional-area varying wind channels to measure the pressure differences within the wind channel on a range of wind speeds. We hypothesize the pressure sensors will be able to accurately measure pressure difference, and that we will be able to use that data to calculate the wind's magnitude and direction using Bernoulli's principle. Throughout experimentation, we develop multiple setups to test the capabilities of the DPS310 sensors. The project is largely exploratory as we investigate the functionality of the pressure sensors in different wind conditions. The imprecision of data collection at lower wind speeds provided difficulties, but the results overall revealed that at high speeds and a small angle of the wind velocity relative to either of the channels, Bernoulli's equation is able to roughly calculate the magnitude of the wind velocity. Due to the rotational symmetry of our device, we are also able to tell the direction of the wind within a tolerance of $\pm 45°$.

2 Introduction

The ability to measure wind speeds has always been considered a given. We can utilize anemometers, wind chimes, wind vanes, etc. to help us estimate the strength and speed of the wind around us. However, the precision of these devices are far from perfect, and if a device has high accuracy and precision, it is typically expensive. As wind is an essential component in understanding weather, we are interested in the possibility of a cheaper device that can properly measure wind. Wind in its most basic components is the difference of pressures in the atmosphere. We observe Bernoulli's Principle, which describes the inverse relationship between fluid velocity and pressure exerted by the fluid. Bernoulli proposed that there had to be some force that would increase the velocity from larger volumes to smaller volumes. Another way to understand this is through the behavior of a river: in a wider region, the flow is slower; however, moving through a tighter region, the flow is greater. With an inverse relationship between velocity and pressure, we can use pressure to potentially effectively measure wind speeds as wind can be considered a fluid. This relationship is founded upon the basic law of conservation of energy. A system isolated from outside factors maintains the same total amount of energy, with energy changing into different forms. Bernoulli's Principle is based on Boyle's law of the inverse relationship between pressure and volume i.e. $P_1V_1 = P_2V_2$. This observation was generalized into the inverse relationship between the rate of flow and pressure. As wind is a type of fluid, we can apply Bernoulli's Principle to our experiment, resulting in the mathematical form of Bernoulli's equation i.e. $P_1 + \frac{1}{2}\rho v_1^2 + \rho g h_1 = P_2 + \frac{1}{2}\rho v_2^2 + \rho g h_2$.

3 Methods

3.1 Hardware Setup

In order to perform pressure readings, we needed to construct a device that would measure and display the data simultaneously. We started on a breadboard with different breakout boards all connected to a microcontroller. A breakout board is a device which takes small sensors, chips or components and fabricates them in a way that is easy to use and connects to an entire circuit. In simple terms, they are small devices that perform one or a few tasks so that when they are connected together in a circuit, they can perform multiple tasks. Our breadboard was assembled with the following components: Arduino Mega 2560, DS3231 RTC, microSD breakout, LCD, TCA9548A multiplex, DPS310 sensors. The Arduino acts as a gateway for hardware and software components to interact. The DS3231 RTC is a real time clock that allowed us to track the times of our trial runs. The microSD allowed us to write and save all of our data locally. The LCD displayed both the counter and time for us to track our trial runs. The TCA9548A allowed us to use multiple DPS310 sensors as it allows a multitude of devices to communicate through the same I2C bus, and the DPS310 sensors measured pressure. After using our breadboard device for our singular wind channel velocity readings and angular dependence, we refined it by graduating to a Printed Circuit Board or a PCB. The PCB allowed our setup to be cleaner and transportable as we needed to move with the wind channels repeatedly and contained the same essential components as the breadboard. In addition to the new PCB, we also created new code to measure and cleanly display all 6 DPS sensors. Our initial code was fairly simple, the bare functionalities that we needed were implemented. Our new code used an extensive *setup* as the wind channels needed to be better managed with the addition of 3 more DPS sensors. *Setup* refers to a part of the Arduino code which establishes that all the components on the breadboard are functioning, and all variables are initialized.

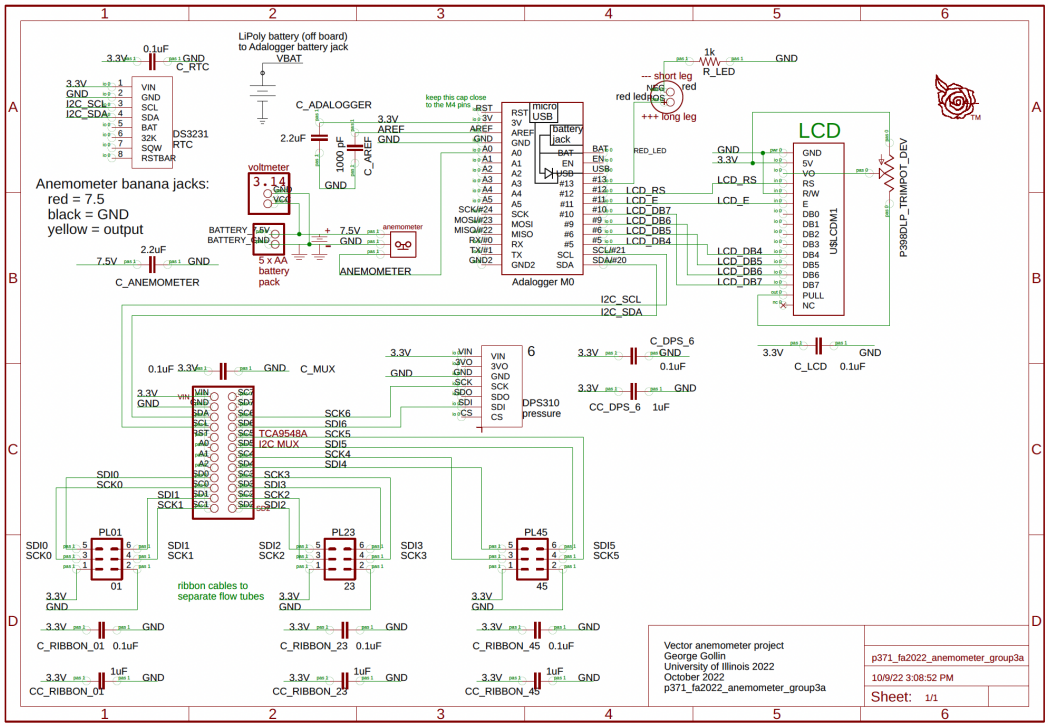

Figure 2: Schematic of the main PCB

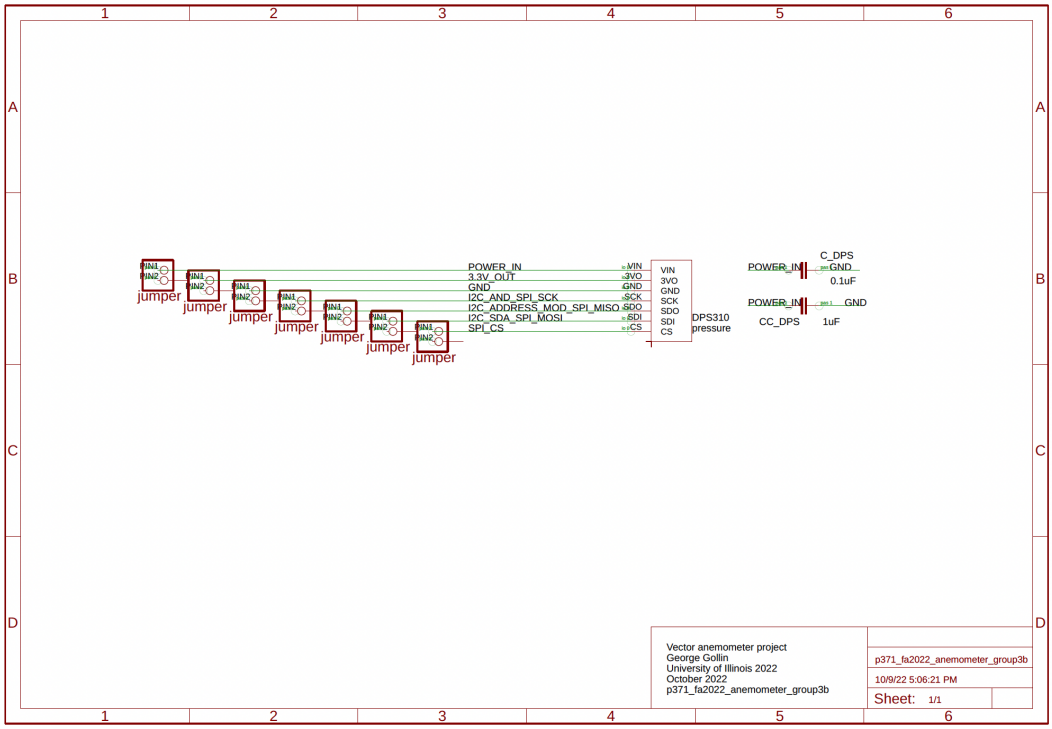

Figure 3: Schematic of the intermediate PCB for the DPS310 ribbon cables

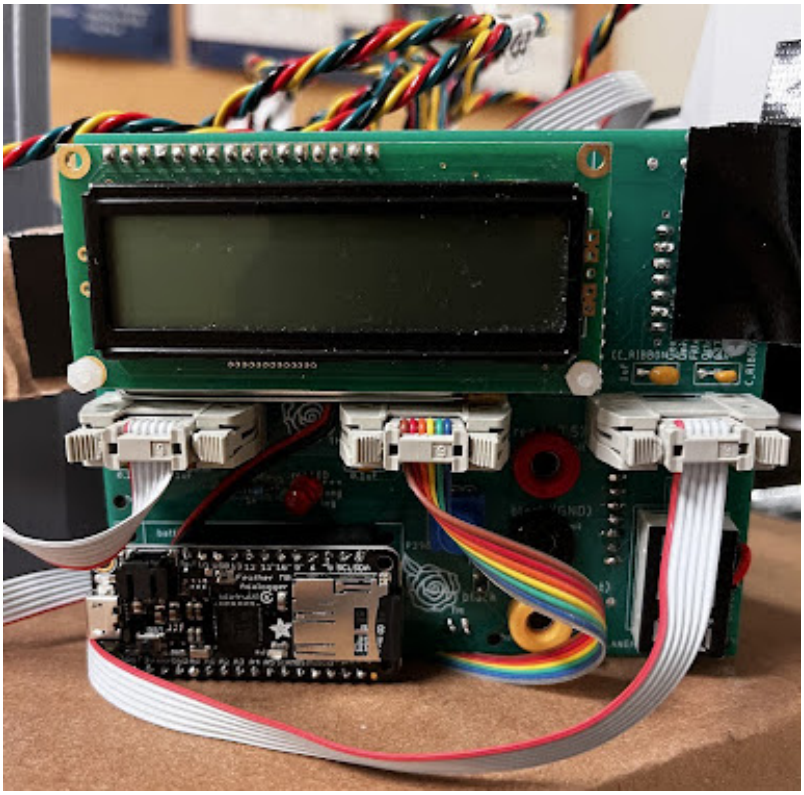

Figure 4: Top side of PCB

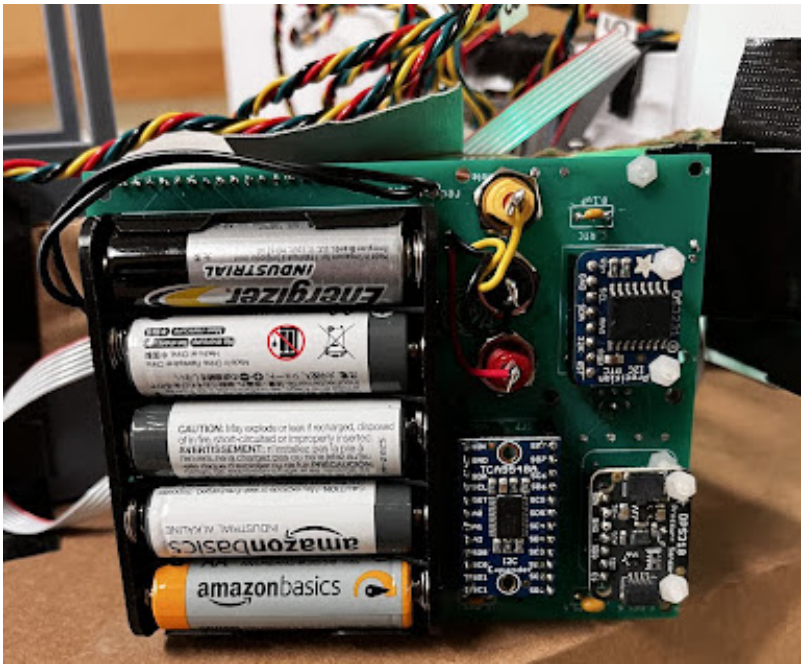

Figure 5: Bottom side of PCB

3.2 Wind Channel Design

The device itself was designed and printed by our team. The varying cross-sectional wind channels were designed using SolidWorks and manufactured with a 3D printer. The design consists of two arms of three chambers each that are attached perpendicular to each other. Of the three chambers in each arm, the inlet and outlet chambers have the same cross-sectional area and the center chamber has a cross-sectional area that is half that of the other two. The two cross-sectional areas are the same for both arms. One arm is attached to the top of the other arm, meaning the top chambers have a slight elevation difference which was assumed to be negligible. Additionally, the top arm was also offset to the side slightly to account for the DPS310 wires exiting from the center of the middle chamber. Connector plates were designed to join chambers within the same arm. The connector plate is a simple rectangle with two clearance holes for an M2 screw. Each chamber included similar clearance holes and all the chambers and arms were put together using M2 screws and nuts.

The biggest factors we kept in mind when designing our wind channels were: ensuring the wind channels were perpendicular to each other, the DPS sensors would fit snug into the wind channels, and that the design would promote proper air flow through the wind channel. In Figure 6, there are several small overlapping structures that screwed into other parts of the wind channel. Screwing it in properly would ensure a stiff connection that would not be easy to rotate. The space for the DPS310 sensors was the only possibility for any leakage. To prevent this, we designed DPS310 carriers that would not only snap onto the DPS310, but also into the wind channels themselves. To further ensure no leakage, we duct taped every area with the potential for leakage as can be seen in Figure 8.

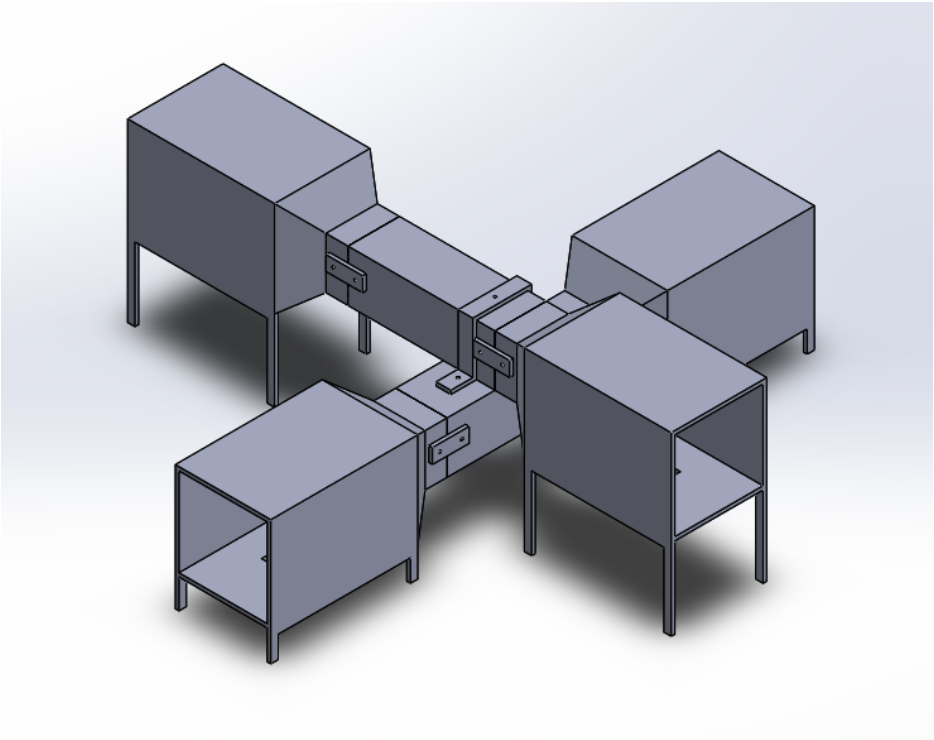

Figure 6: 3D setup designed in SolidWorks

Figure 7: DPS310 carrier piece, manufactured using a 3D printer

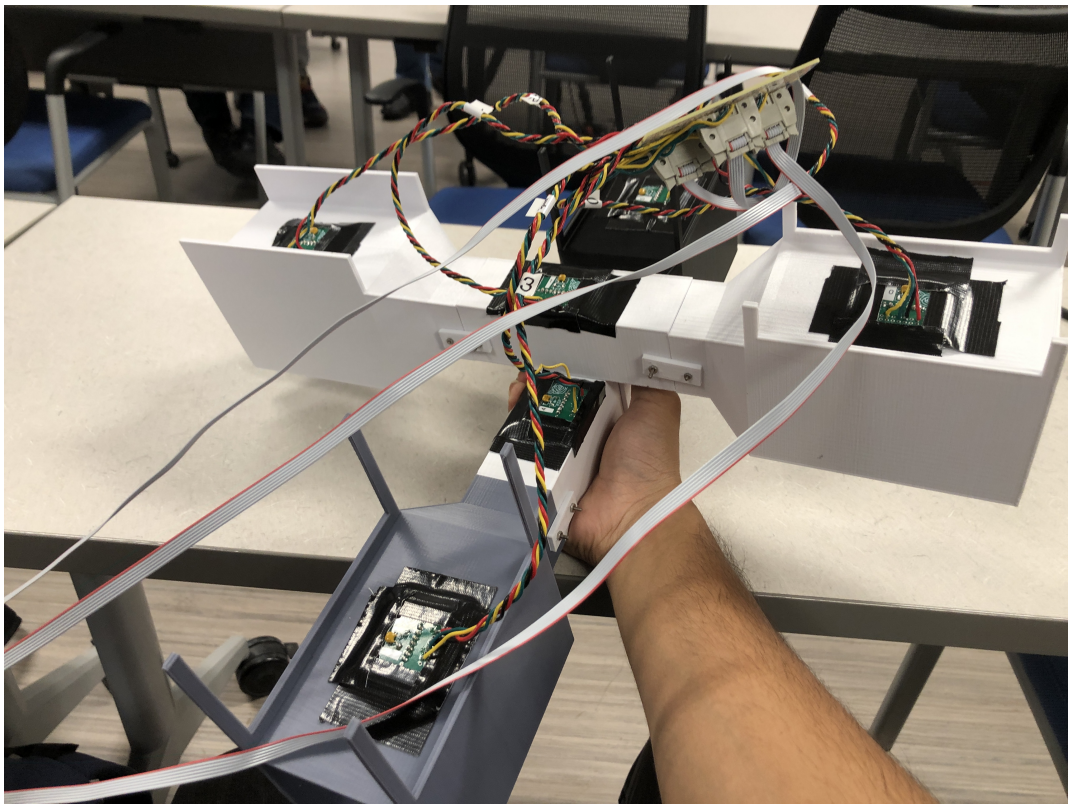

Figure 8: The underside of the full setup showing installation of the DPS310s and connection to the PCB

3.3 Car Setup

Our first experimental setup was driving a car with our wind channel and cup anemometer outside the window. Using the car's speedometer, we monitored the speed of the vehicle to ensure a constant velocity to compare to. The setup required a straightaway that would allow the vehicle to travel straight without veering off course or turning due to obstacles. The setup also included a large empty space that would allow the car to travel in a circular motion, again without any obstacles in the way. Both variations were done at 3 constant velocities: 5 mph, 10 mph, and 15 mph. In order to prevent outside variables from affecting the measurements, we tested the car setup on days with low wind speeds, and ensured we were traveling the same direction for both the line (east to west) and circle (counterclockwise).

Figure 9: Experimental setup of the calibration test using a car

3.4 Box Fan Setup

Our second experimental setup used a box fan and our wind channel in a stable environment. The wind channel was set up directly in front of the box fan. The wind channel was rotated from 0° to 90° in 10° increments. In order to maintain a stable wind flow for the wind channel, one end of the wind channel was centered according to the box fan for the entire experiment. The fan had 3 different speeds that were tested for each angle.

Figure 10: Testing angular dependency in one axis

3.5 Hallway Walk Setup

In our final setup, we used an empty straight hallway, and a stable platform for our device. To prevent human error, we utilized a cart on which our device could travel on through the hallway. We measured out a fixed distance as well as set certain time intervals to maintain around a certain speed. The distance was 30.5 meters, and the 3 approximate speeds were $2\frac{m}{s}$, $1.3\frac{m}{s}$, and $1\frac{m}{s}$. For the cart setup, we started with an arm facing parallel to the length of the hallway. We set the parallel arm as 0° in our measurements. To check angular dependency with both wind channels, we rotated the wind channels by 5° until 45°. In a separate test, to ensure that our device was rotationally symmetric, we started at 0° and rotated the device to 180° in 45° increments.

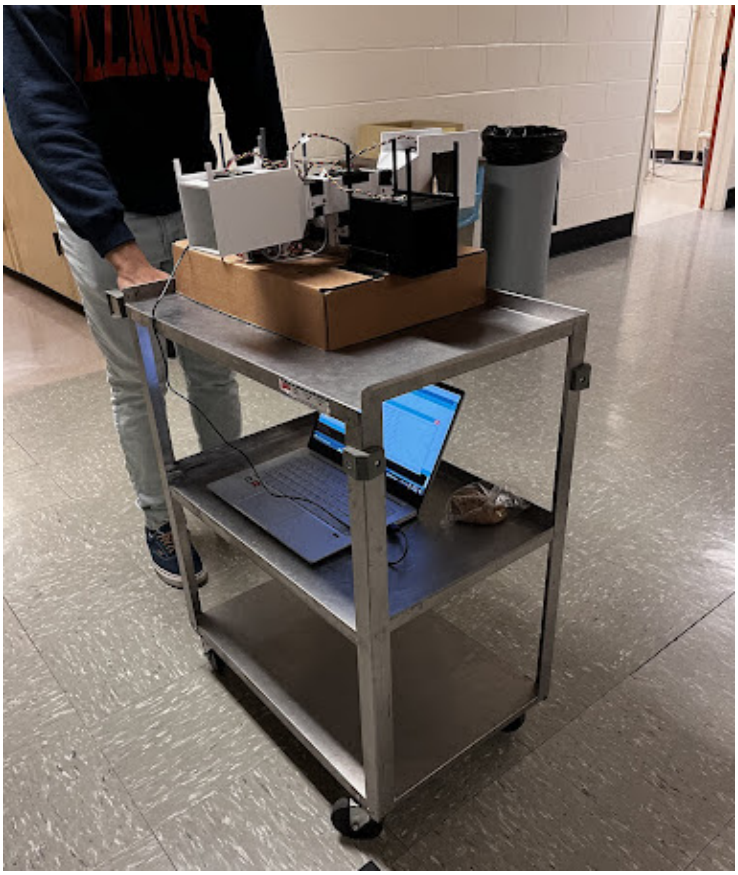

Figure 11: Testing the device's angular dependence using a straight hallway

4 Experimental Design

Our experiments had two foci on Bernoulli's Principle: calibration and angular dependence. To properly determine the angular dependence, we had to calibrate the devices we were using to see if our results were accurate.

Our first setup, the car setup, had the sole task of calibrating both the wind channel and the anemometer. The car was a simple choice as the box fan did not have any written measurements of its velocity at low through high speeds. Utilizing the car speedometer, we had a value to compare both the cup anemometer and the calculated velocity from the wind channel to. In the car setup, we drove both in a straight line and a circle to understand noise and percent error in our data from the DPS310 sensors.

The box fan setup focused mainly on the angular dependence of a singular wind channel. Since the pressure differences from 90°-180° would be symmetrical to 0°-90°, we tested up to 90°. Testing a single wind channel's angular dependence would allow the data analysis to be significantly easier, going through 3 pressure sensors versus 6. While previously we used the cup anemometer, we solely used the wind channel and its DPS310 sensors in measuring angular dependence of the single wind channel. From the first set up, we understood that we could use solely the pressure differences to calculate the velocity within the chambers.

The hallway walk setup concentrated on the angular dependence of both wind channels. While the box fan was formerly used for a single wind channel, the fan was not wide enough for us to comfortably use it for 2D angular dependence. Using the hallway and a cart would allow us to be in a better controlled stable environment for the pressure sensors.

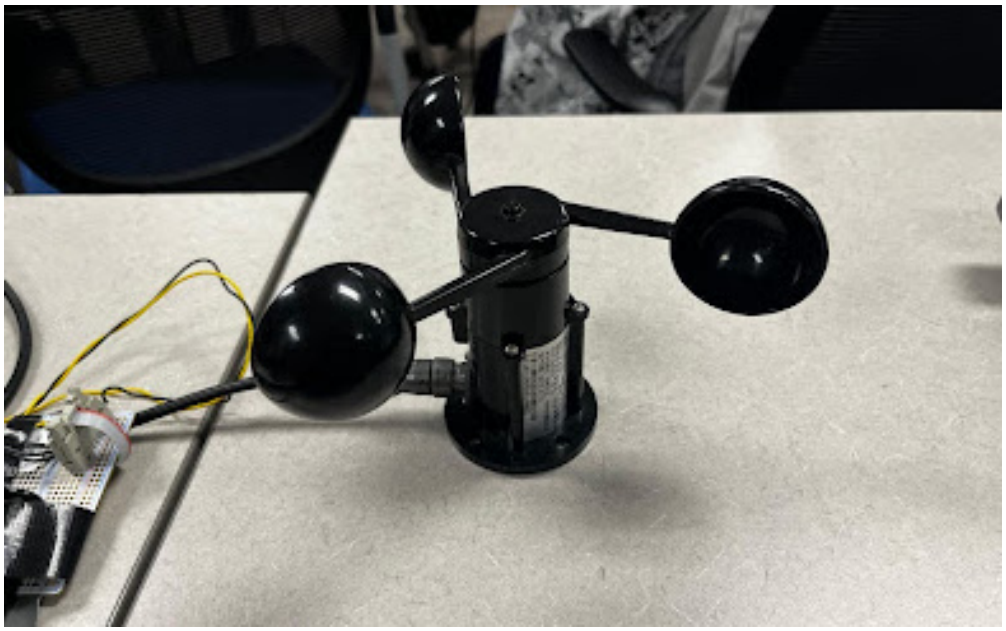

Figure 12: Cup anemometer attempted to be used for calibration

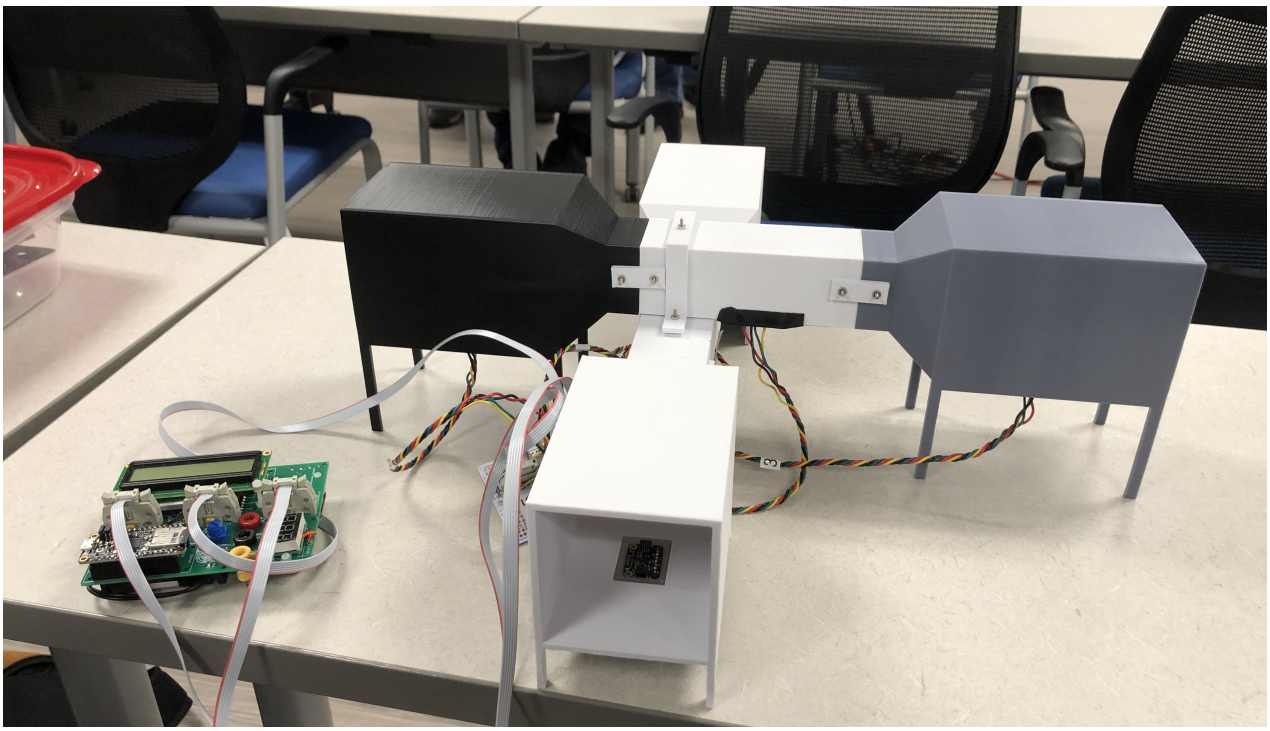

Figure 13: Full setup of our device including the PCB

4.1 Assumptions and Variables

When doing our calibration tests, we outside wind velocity was present but accounted for as we zero out each sensor's pressure readings with an ambient pressure. This is further ensured through driving in a circle, where wind velocity in various directions would theoretically cancel out, and driving in the same direction when going in a straight line, the wind would affect each test equally. Since Bernoulli's Principle utilizes fluids, we had to make the assumptions required to use Bernoulli's Principle. This includes the fluid being incompressible, the flow being inviscid, the flow being steady and laminar, and the flow being two-dimensional. An incompressible fluid means that the density stays constant with time. In fluid mechanics, most liquids are generally considered to be incompressible, while gases are typically considered to be compressible. However, since all tests we conducted were done at relatively low speeds, we believe this assumption is justified.We assumed the density of air to be $\rho_{air} = 1.122\frac{kg}{m^3}$. We also assumed a constant dynamic viscosity of air to be $\mu_{air} = 18.6 * 10^{-6} Pa \cdot s$. An inviscid flow is an ideal condition in which we assume the fluid does not have any friction losses. A steady, laminar flow means that the flow does not have a time dependence; if we set up the experiment and come back some time later, the flow should be the exact same.

Every lab experiment contains a plethora of variables, but in order to simplify our data reduction, we simplified the variables considered in the experiments. Our control variables were the density and dynamic viscosity of air. Our dependent variable was the measured pressure values from the DPS310s and the voltage values from the cup anemometer. Lastly, our independent variable was the wind speed.

5 Discussion and Results

5.1 Car Calibration Data

Throughout our entire data analysis, the main equation we used was the equation for the velocity in the middle chamber of an arm which was derived from Bernoulli's Principle. We start with Bernoulli's Principle written as such:

$$P_1 + \frac{1}{2}\rho v_1^2 = P_2 + \frac{1}{2}\rho v_2^2$$

In the above equation, P is pressure, ρ is density, and v is velocity. Point 1 in this equation is taken to be the bigger inlet chamber, while point 2 is taken to be the smaller outlet chamber. We disregarded the elevation difference due to the fact that the center of both chambers were at the same vertical distance. In order for us to simplify the equation above we have to use the conservation of mass. Specifically, we know that whatever goes in the arm must come out. This means that the flow rate, $\dot{Q}$, must be a constant. Therefore we get the following equation:

$$\dot{Q} = v_1 A_1 = v_2 A_2$$

In this equation, v is velocity and A is cross-sectional area. The area of the outer chamber is four times greater than the that of the middle chamber, meaning $v_1 = 0.25 v_2$. Substituting this into our simplified Bernoulli's equation and reformulating gives us the formula for the velocity in the middle chamber:

$$v_2 = \sqrt{\frac{P_1 - P_2}{\frac{15}{32}\rho_{air}}}$$

The only other equation used in our data was the equation for the Reynolds number which is used to determine how laminar or turbulent the flow is. The equation is as such:

$$Re = \frac{\rho v L}{\mu}$$

In this equation, ρ is density of air, v is velocity of air, L is characteristic length (which, in our experiment, is the width of our chamber), and μ is the dynamic viscosity of air.

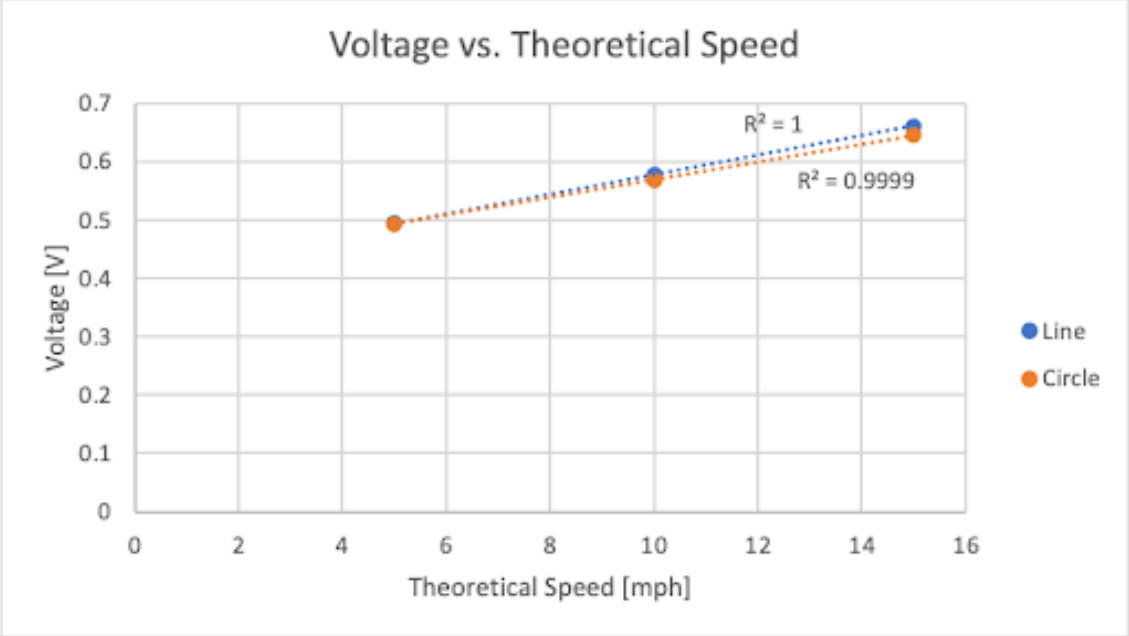

Figure 14: Voltage vs. theoretical (car) speed for circle and line test with data averaged over time, test 1

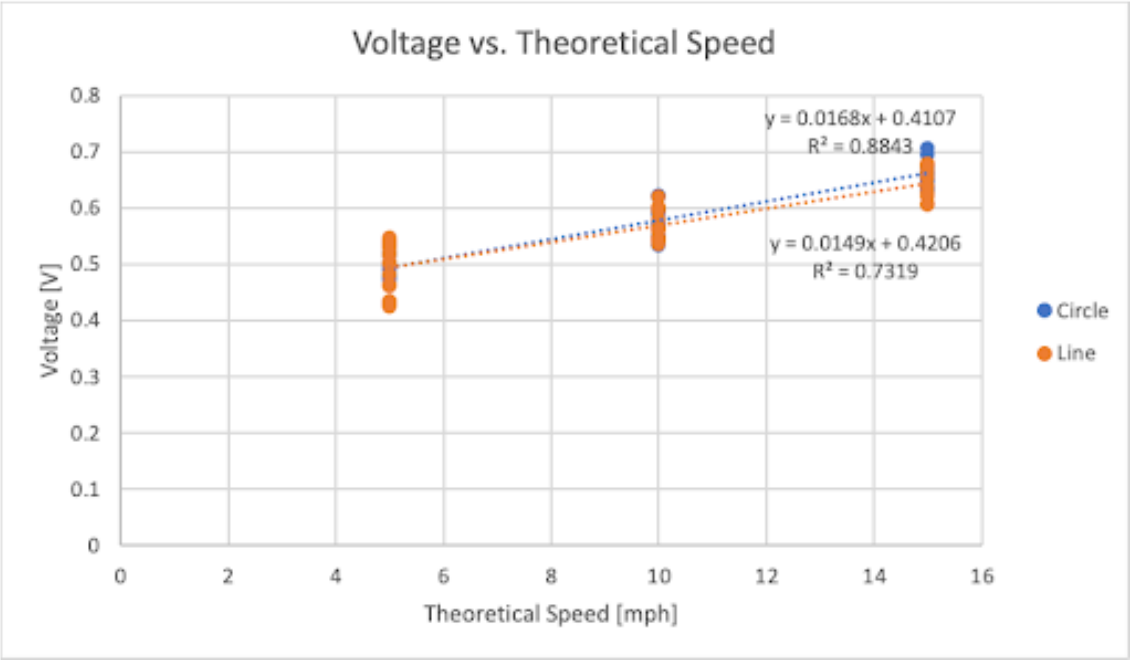

Figure 15: Voltage vs. theoretical (car) speed for circle and line test with data split into 5 second intervals, test 1

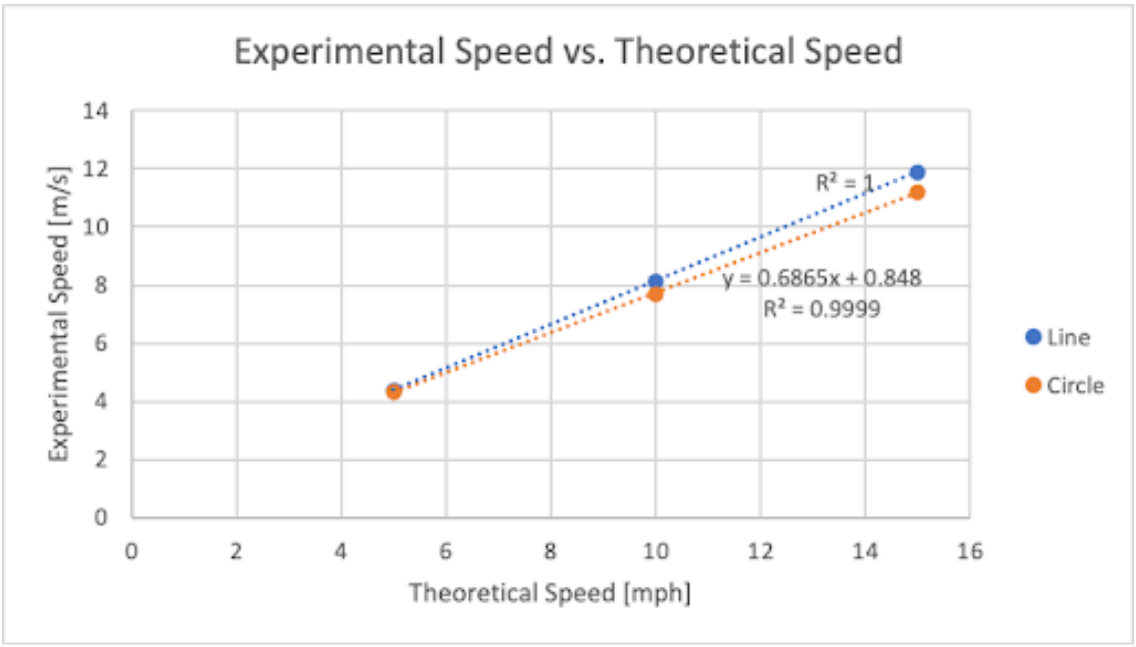

Figure 16: Experimental speed from cup anemometer vs. theoretical (car) speed for circle and line test, test 1

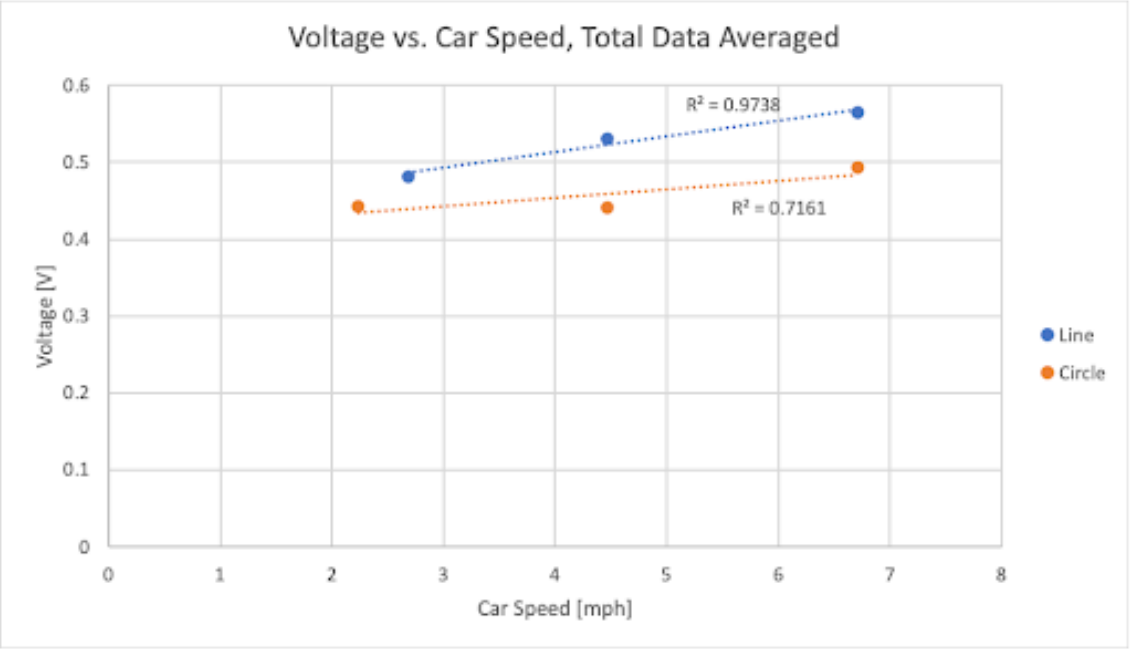

Figure 17: Voltage vs. car speed for the line and circle test with data averaged over all time, test 2

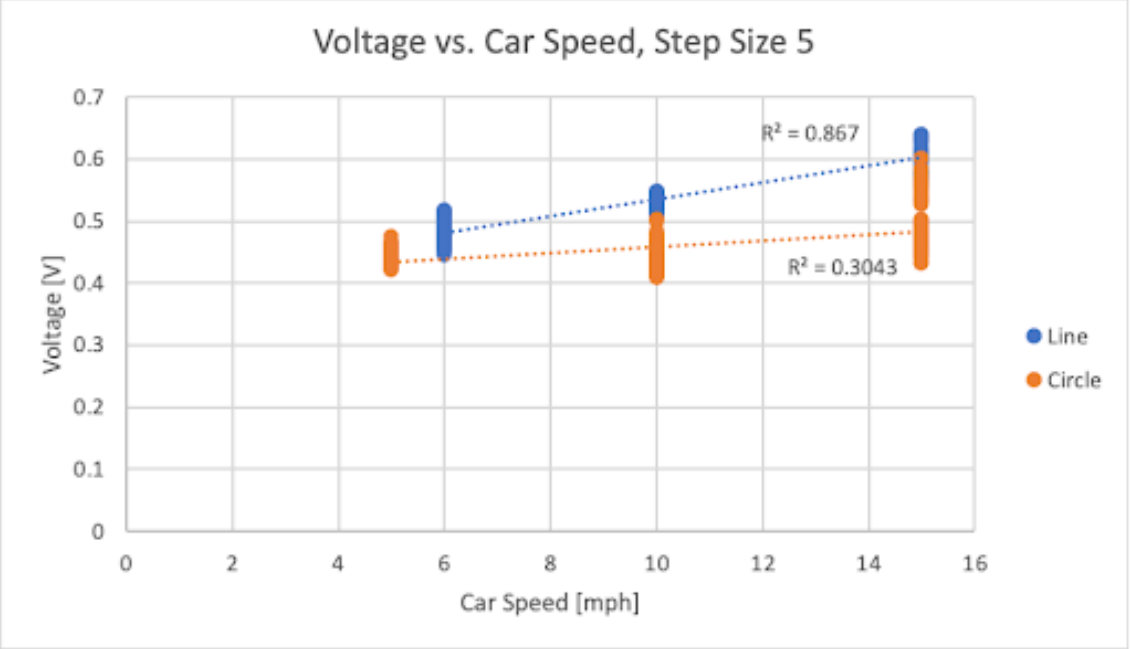

Figure 18: Voltage vs. car speed for the line and circle test with data split into 5 second intervals, test 2

To begin our analysis, we took the averages of the cup anemometer voltage over the entire interval for each lap and plotted them against the speed of the car. Figure 14 and Figure 17 show the results of two different tests, but Figure 14 specifically was very alarming. No matter how perfectly we could collect the data, we would never expect an exact correlation between variables, especially given our monitoring of the serial monitor mid-testing. This prompted us to search for possible errors, leading us to divide up the interval. This was done to avoid giving the average too much power in masking the noise of our system. We chose new intervals of five seconds and plotted the averages over them. This was much more revealing. As seen in Figure 18, the line tests retained a reasonable R^2 value, but the circle test, at .3043, shows a very poor correlation. This was in line with our qualitative observations during the recording process. We noticed multiple times where the cup would slow, reverse directions, or completely stop while the car was still in full motion, moving in circles. Due to the inconsistencies in our data with the cup anemometer and a general inability to calibrate it, we were forced to conclude that the wind profile around the car was simply too complex to use the cup anemometer.

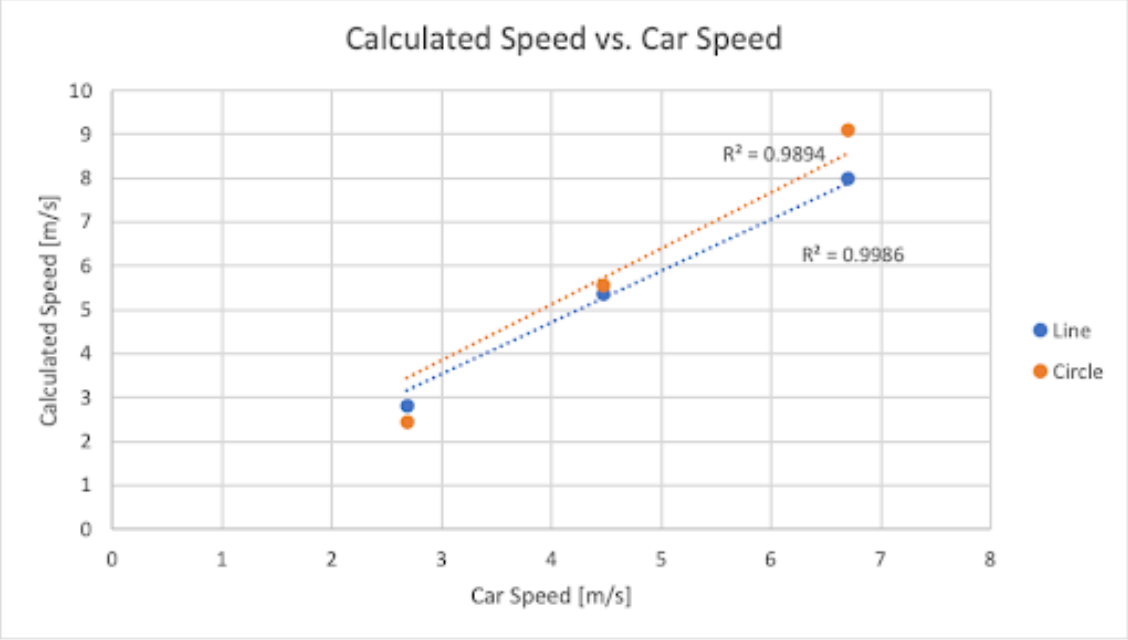

Figure 19: Calculated speed using DPS310 data vs. car speed for line and circle test with data averaged over all time.

Overall, the DPS310s proved to be much more consistent than the cup anemometer. Once again we took averages over the entire interval. We obtained a very high R^2 value, but not an unbelievable one like in the case of the cups. These were promising results, and suggest that the wind channel is sensitive enough to measure velocity, at least in the case of parallel flow and high speeds. As far as calibration, the strong correlation and lack of constant offset or multiplicative factor implied very little calibration was needed for the device. We noticed that the middle chamber seemed to match the outside velocity the best, while the front chamber was about a fourth of that. The back chamber seemed completely unrelated to the other two, which is very interesting and currently unexplained. From Bernoulli's Principle alone, we would expect the back speed to match the front speed because they share the same cross-sectional areas, but there are clearly confounding factors at play.

5.2 Box Fan 1D Angular Dependence Data

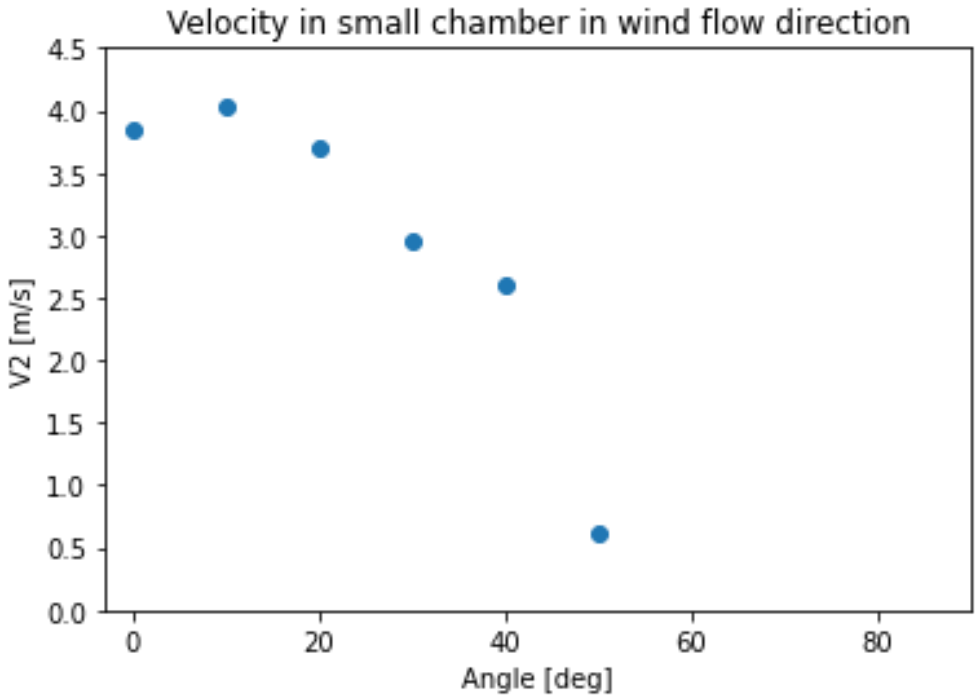

Figure 20: Velocity in the middle chamber vs. angle for the box fan's highest speed

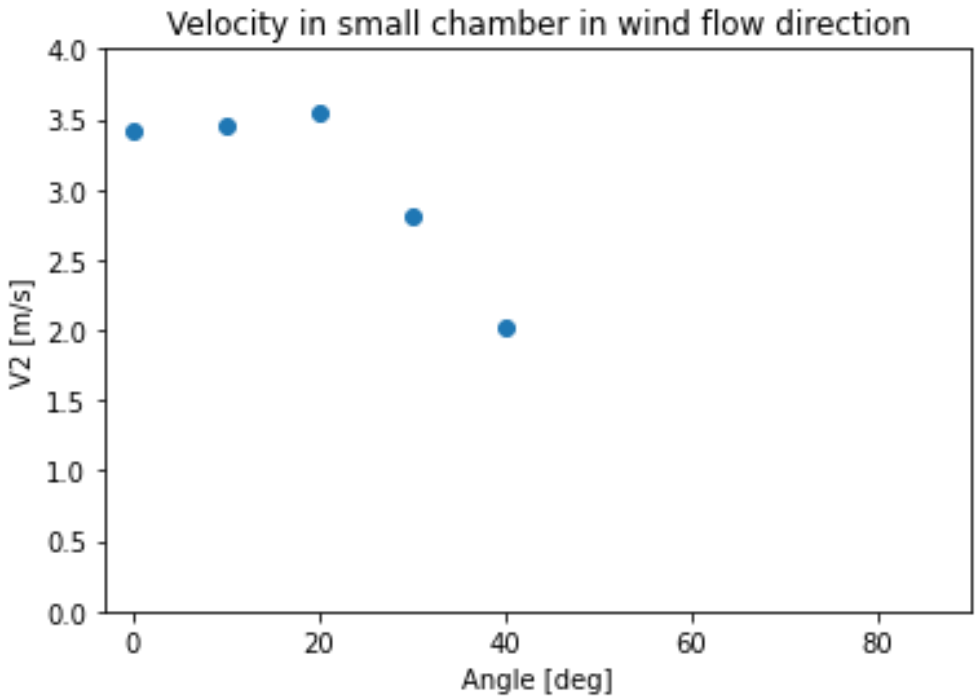

Figure 21: Velocity in the middle chamber vs. angle for the box fan's medium speed

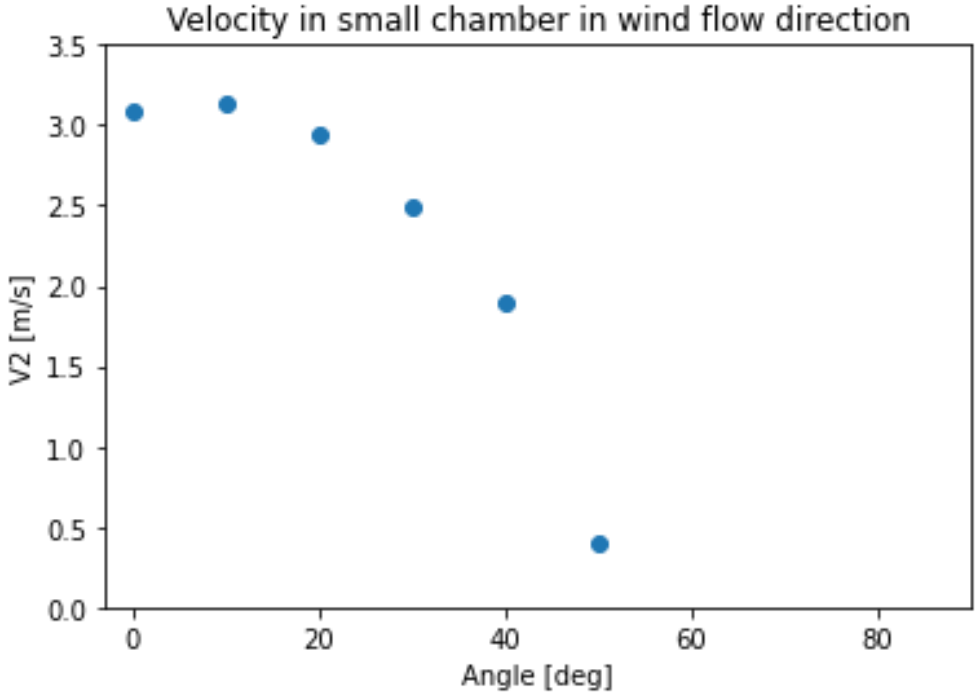

Figure 22: Velocity in the middle chamber vs. angle for the box fan's lowest speed

To further our investigation we wanted to test the device's angular dependence. If our device was perfect and Bernoulli's Principle held, we would expect a plot of velocity vs. angle to look like a cosine curve. It was evidently not that simple, although Figures 15-17 are very self consistent. First, the plots all look roughly like the first quarter of a cosine curve, as hoped. The biggest discrepancy is that the peak velocities are never at 0°. We are unsure of why this is, but the consistency of this discrepancy suggests that there was some sort of systematic experimental error occurring. The difference is not drastic however, so it is still plausible to propose a cosine relationship. However, the real oddity is around 50°-60°, where the plots cut off. Data was recorded up until 90° for each figure, but the pressure differences end up negative at 60°, 50°, and 60°, respectively. What this means is that the velocity equation derived earlier returns an imaginary value and further, Bernoulli's Principle fails to describe the dynamics of the system past this point. This cutoff seems to be arbitrary, but it's likely the system simply requires small angles.

5.3 Rotationally Symmetric Test Data

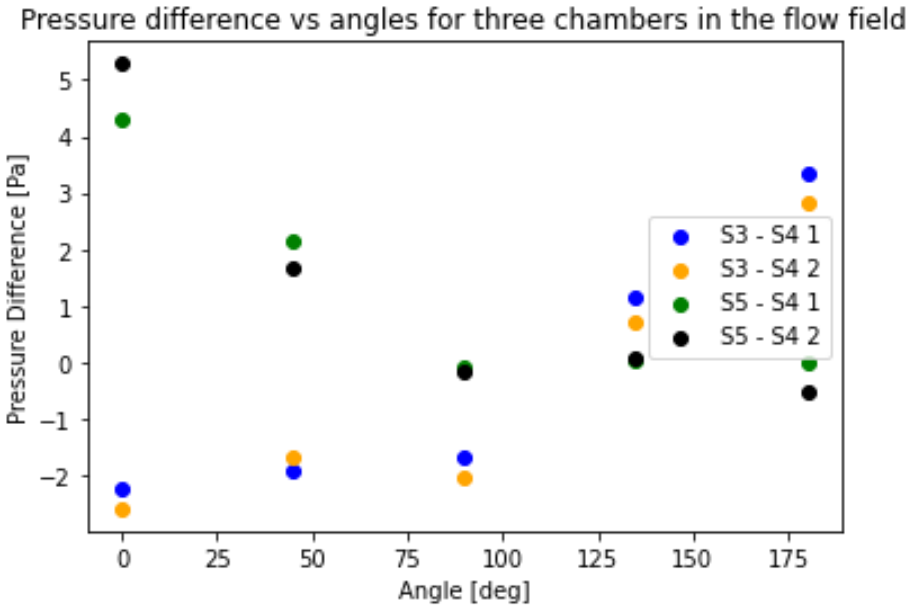

Figure 23: Pressure differences plotted against angle for the Sensor 3-4-5 axis including both the front and back differences

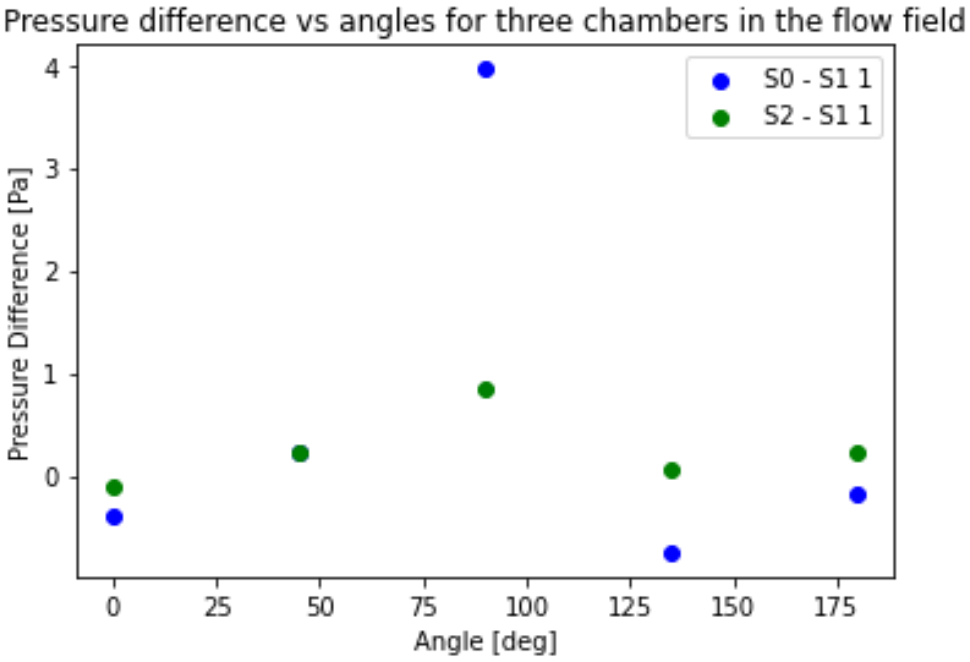

Figure 24: Pressure differences plotted against angle for the Sensor 0-1-2 axis including both the front and back differences

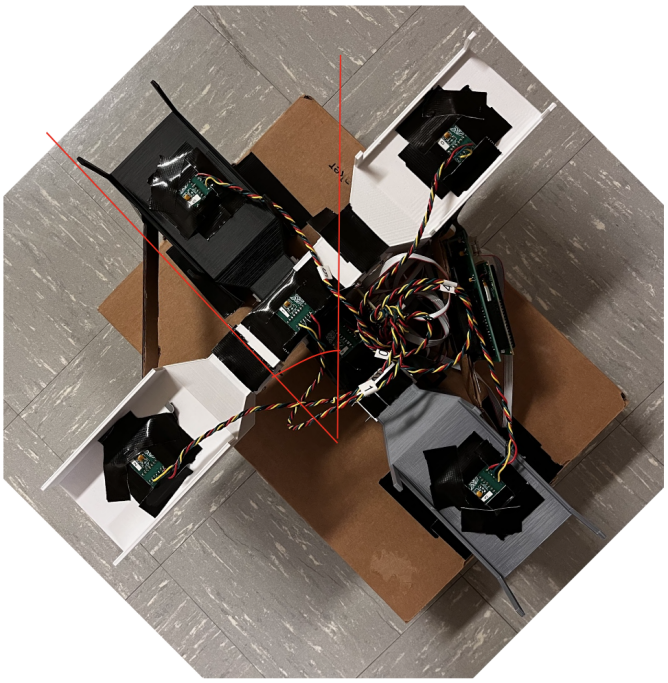

Figure 25: Overhead view of the device at one possible 45° orientation.

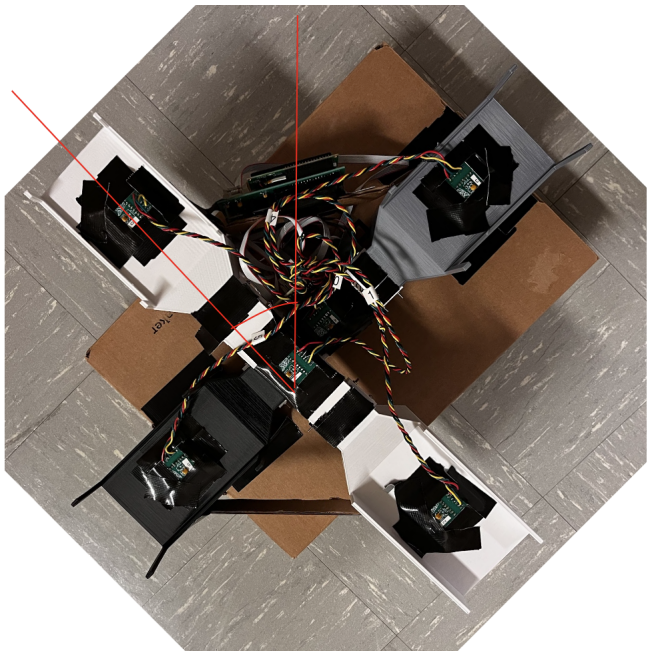

Figure 26: Overhead view of the device at another possible 45° orientation.

One necessary property for the device to have any merit is rotational symmetry. The final data on the wind should not depend on the order of the sensors. For example if we were to run the same trial in the orientation in Figure 25 and the orientation in Figure 26, we should get the same results for wind speed and direction.

To test this we went from 0° to 180° in 45° increments, starting with sensor 5 in front, and doing each angle twice. In these figures, the angle is measured with respect to the starting point, where Sensor 5 was in front. From Figure 23, we can see that the device exhibits symmetric behavior. The difference from Sensor 5 starts highest, decreases on a curve, then fluctuates slightly as it approaches the back position. The difference from Sensor 0 starts lowest, fluctuates slightly, then increases on a curve as it approaches the front position. The fluctuations in Sensor 0 at 0°, 25° and 90°, along with those in 5 at 90°, 135°, and 180° can be explained by the earlier note that Bernoulli's Principle does not seem to apply to the chamber in the back of the device. One new concern the plot raises is that there seems to be an offset between the devices. One would expect,

for instance, at 90°, for the values to be the same since both chambers would be perpendicular to the wind flow. Here we see the sensor 5 data is higher, but this is likely experimental error, as a similar trend is not seen in our other trials. From the shapes alone though the curves clearly show rotation symmetry.

Figure 24 shows data from the axis initially perpendicular to the flow, which once again reaffirms the symmetry. At 0° the 2 pressure differences are very close, which makes sense because the axis is perpendicular. The points then rise to a peak at 90°, where Sensor 0 is now the front facing sensor, and the peak is a very similar value to the peak of Sensor 5. The values cannot be directly compared because of slight variations in walking speed between angles. The curve then follows a similar shape down as the way up, with one outlier point, returning to orthogonality.

What this rotational symmetry allows us to do is predict the direction of wind to ± 45° accuracy. We can identify the axis that has the highest pressure difference, and then identify a "front" and "back" chamber based on which has the higher pressure difference. We then claim the wind is coming from that direction, ± 45°. The ± arises from the symmetry, as symmetry would require the axes to appear equal if they were both 45° to the oncoming wind. However, 1° towards one axis would make its pressure difference appear greater. We therefore cannot claim the velocity is entirely along the axis just by observing a greater difference.

5.4 Hallway Setup 2D Angular Dependence Test Data

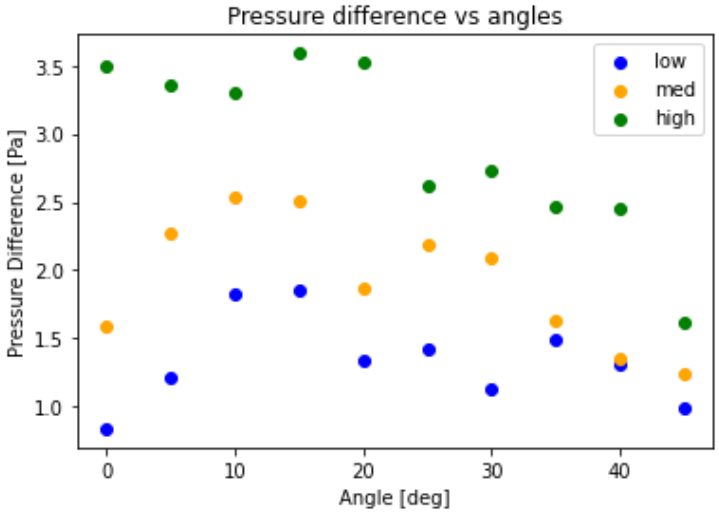

Figure 27: Pressure difference in the forward facing arm between the inlet chamber and the middle chamber as a function of angles

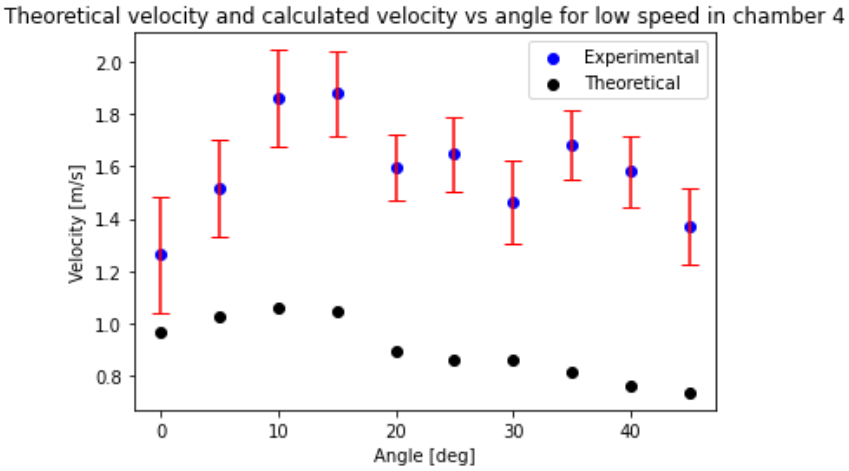

Figure 28: Theoretical velocity and calculated velocity from Bernoulli's equation in the middle chamber of the arm that is initially parallel to the wind at a low speed as a function of angle with error bars on the calculated velocities

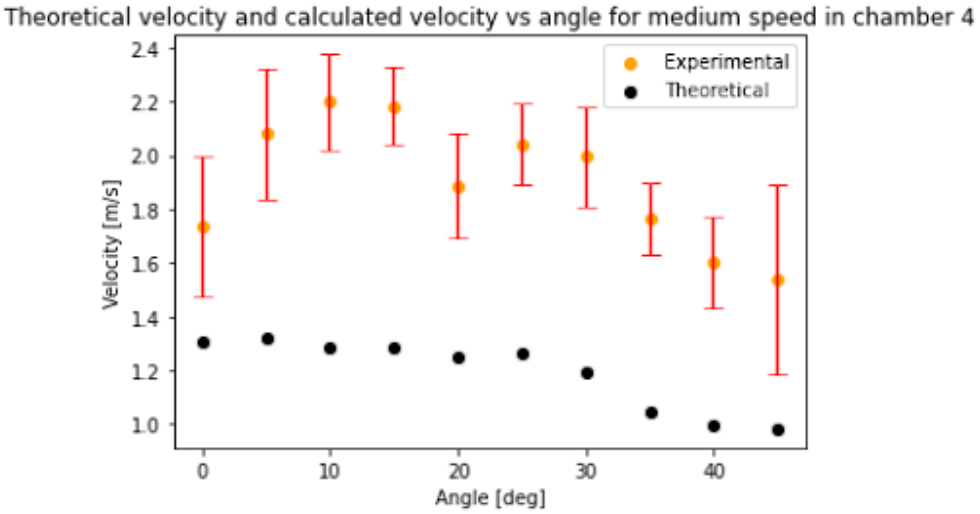

Figure 29: Theoretical velocity and calculated velocity from Bernoulli's equation in the middle chamber of the arm that is initially parallel to the wind at a medium speed as a function of angle with error bars on the calculated velocities

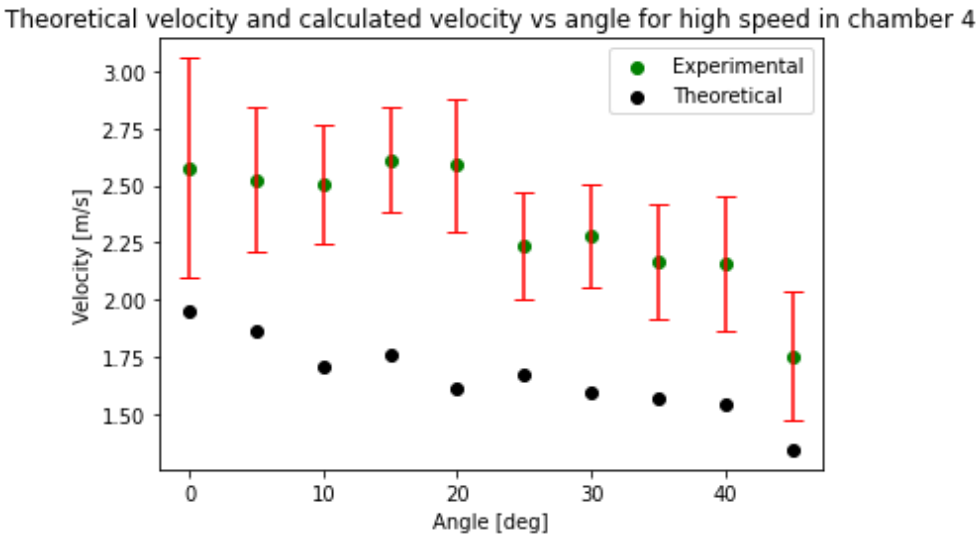

Figure 30: Theoretical velocity and calculated velocity from Bernoulli's equation in the middle chamber of the arm that is initially parallel to the wind at a high speed as a function of angle with error bars on the calculated velocities

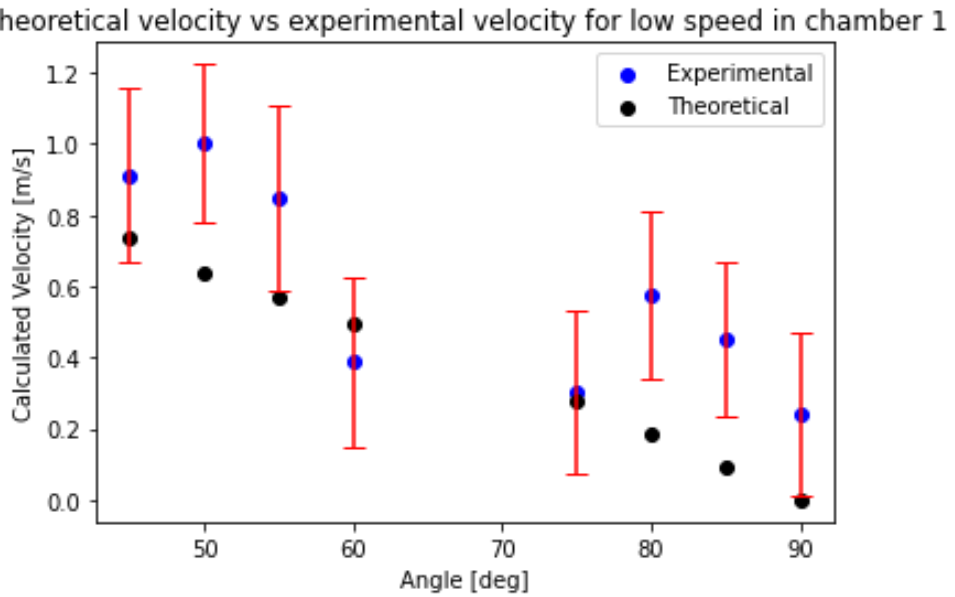

Figure 31: Theoretical velocity and calculated velocity from Bernoulli's equation in the middle chamber of the arm that is initially perpendicular to the wind at a low speed as a function of angle with error bars on the calculated velocities

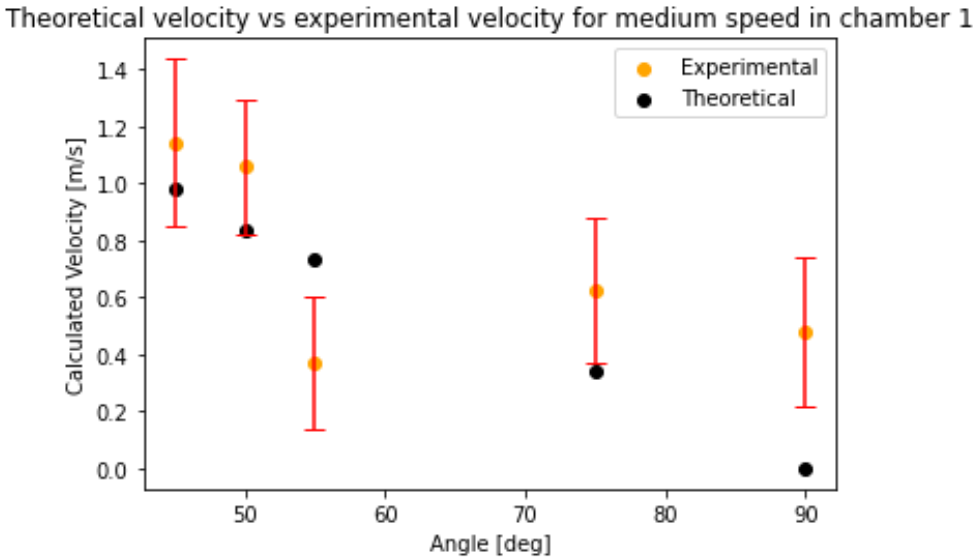

Figure 32: Theoretical velocity and calculated velocity from Bernoulli's equation in the middle chamber of the arm that is initially perpendicular to the wind at a medium speed as a function of angle with error bars on the calculated velocities

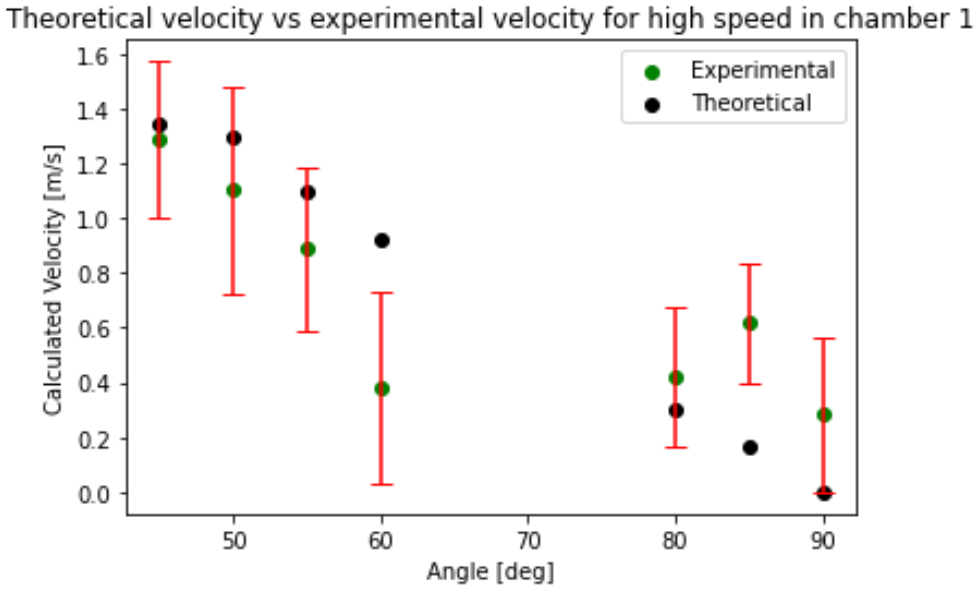

Figure 33: Theoretical velocity and calculated velocity from Bernoulli's equation in the middle chamber of the arm that is initially perpendicular to the wind at a high speed as a function of angle with error bars on the calculated velocities

To finalize our analysis we performed a fine tuned sweep through the angles with 2 axes, with a broad overview of the results shown in Figure 23. Importantly, although we tried to be as close as possible with speed between trials, there was some natural variation. This directly affects the shape of the curves, but general trends can still be observed. Notably, the pressure differences are always higher at higher speeds, regardless of the angle, as it should be. Something else to note is that both medium and low speeds have local minimums at 0°. This is strikingly similar to the earlier analysis with the box fan, although the effects are slightly more pronounced here. What is promising however, is the pressures at high speed. The 0° point is much higher up relative to the others, only outshined slightly by outliers at 15° and 20°, which can easily be explained by our velocity variation. This, in combination with the earlier results of the car trials, suggests that the device can handle higher speeds much better than lower ones.

In Figures 24-26, we look at the axis originally facing parallel to the flow. The varied speed in between angles is now accounted for, as we plotted our actual speed at each angle times its cosine in order to pick out the velocity component along the axis. We then plotted the calculated velocity along with its standard deviation as error bars. The resulting plots are seemingly strong evidence against the reliability of Bernoulli's Principle. None of the angles at any of the speeds have close enough points to have the theoretical values inside the error bars of the calculated values. However, they are not entirely counterproductive. Comparing the max distance between error bar and theoretical, low and medium speed are $\sim$.7 m/s away while high is $\sim$.6 m/s away. This tendency towards higher accuracy at higher speeds strengthens the previous trends.

In Figures 27-29, we look at the axis originally perpendicular to the flow, with the same set of variables. These are very interesting, as many of the points are within a standard deviation of the actual values. Considering that this axis started at 90 degrees however, this result is not at all expected. In fact, that there are so many values at all is contrary to the box fan trials. While still

there, there are far fewer points that had to be cut out due to being imaginary, and somewhat surprisingly, it's still in the middle range of angles, not at the very end. Based on previous results, we would've expected the plots to drop off around 50-60 degrees and still have an offset between the standard deviation and theoretical value before then. Due to this surprise we can say that Bernoulli's Principle is, at best, inconsistent in its description of our device.

6 Difficulties and Complications

In order to get a baseline velocity to compare our results to, we utilized a cup anemometer to accurately measure the wind speed of the box fan, outside of a car, etc. After multiple attempts to calibrate the cup anemometer, we found anomalies that were not accurate with the wind speed we were averaging. During the anemometer calibration, the anemometer was not consistently showing 0 mph despite no movement from the cup anemometer. This inaccuracy led our comparison between the theoretical velocity and experimental velocity to be confusing as there did not seem to be a proper correlation. After weeks of attempting to calibrate and utilize the anemometer, we dismissed the idea of using the cup anemometer and turned to solely using the pressure differences within the wind channel's chambers.

During our initial trials, our group designed a breadboard to run all the basic functions. We had the DPS, LCD, RTC, etc. attached on the breadboard, with code that was designed specifically for the Arduino and breadboard. Once we had our full cross sectional wind channels, we needed a PCB to handle the multitude of DPS sensors as well as the ribbon cables through it. This would allow a compact circuit board that would be transportable with the wind channels. With the changed design in the PCB, our original code was not fully functioning with the PCB. We were unable to troubleshoot our code and make it compatible with the PCB, thus we had to discard the code altogether. This setback was difficult to work with as we were already several weeks into calibrating and testing. Professor Gollin helped develop a new code that was fully functional with the PCB.

After testing the box fan setup with a singular wind channel, the box fan width and area of the setup was not large enough for both wind channels to be properly measured. After an attempt with the box fan, the wind channels were hanging off the table. The car was also not a possible option as holding both wind channels out the window was not plausible and maintaining the rotated

wind channels would also be difficult. We conceptualized another method, walking through the hallway, to test the angular dependence of both wind channels. This would allow our device to easily maintain any angle it was switched to, as well as fully receiving the air flow through the chambers.

7 Conclusion and Future Work

In this lab, we explored the possibilities of using DPS310 sensors to build a vector anemometer using pressure differences to calculate wind magnitude and direction. Utilizing a breadboard and PCB, we constructed our own cross-sectional-area varying wind channels to measure the pressure differences. Through the car trials, we found a strong correlation between higher wind speeds and the calculated wind speed through the pressure sensors. The speed factor, which is the ratio between the calculated speed and theoretical speed, at a lower speed was ≈ 1.78 and as we increased the speed, the speed factor decreased down to ≈ 1.4. For reference, the closer to 1 the speed factor is, the more accurate. Through the other setups, box fan and hallway, we saw a lower correlation between the theoretical and actual velocity magnitude. This was due to the fact that our highest speeds in these setups were similar to the lowest speed of the car setup. Not only that, the difference between the high speed and low speed trials of the hallway setup was significantly less than the difference in the car setup. Despite the lack of accuracy with magnitude, a strong correlation was shown between velocity direction and an angular rotation with a tolerance of $\pm 45°$. Our plots, relating angular dependence to velocity, showed a curve of best fit similar to a sinusoidal function, which is what we theorized. The speed factor further relates higher speed to accuracy within the perpendicular wind channel, with low speeds having a speed factor of ≈ 1.54 and high speeds having a speed factor of ≈ 0.88. All of our data allows us to conclude that with high speeds and small angles of the wind relative to the channels, one may be able to calculate wind velocity using the DPS310 pressure sensor and Bernoulli's equation.

Moving forward, many small improvements could have been made to our device and our experimental setups. Understanding the importance of speed distribution could have changed our results greatly. Utilizing the car and a platform that could hold the wind channels outside the car window would have allowed us to experiment with greater speeds, and potentially see a stronger correlation between both the experimental wind vector and the theoretical wind vector. In addition to

using higher speeds, we believe using a diffuser would allow us to get a more laminar flow, and thus more accurate results. However, with the design of a rectangular plane as a chamber of the wind channel, we are able to stay in range of laminar flow according to our Reynold's number. For all our experiments, we calculated the average Reynolds number to be $Re = 3012$. For flow that is travelling along a rectangular plane, the critical Reynold's number that dictates when flow transitions from laminar to turbulent is roughly $Re = 500,000$.

For a pressure sensor that is as cheap as \$7.50, a device such as our opens the accessibility of measuring accurate wind vectors. Being able to accurately measure wind would allow people such as small-sized farmers to better prepare their crops for strong wind conditions, allowing them to plan accordingly and protect their plants. It also creates accessibility for people to understand and predict weather patterns, giving people a chance to explore a field they would not be able to otherwise. These cheap devices with great power present tremendous potential and opportunities that can be used to benefit the future of many.

8 Acknowledgements

Our group would like to personally thank our Professor George Gollin as well as our teaching assistant Anthony Mirasola. They provided tremendous input to ensure we completed our lab on time. Throughout our experimental flaws and coding errors, Professor Gollin went the extra mile and led us in the right direction to solve these errors. Anthony Mirasola helped us understand Bernoulli's Principle as well as other misconceptions in depth. We would also like to give extreme gratitude to Professor Gollin for designing our PCB, allowing our device to be fully transportable, making data acquisition significantly easier.

9 References

1. "Bernoulli's Equation." *Encyclopedia.com*, Encyclopedia.com, 1 Dec. 2022, www.encyclopedia.com/science-and-technology/physics/physics/bernoullis-principle.

2. "DPS310 Digital Barometric Pressure Sensors." *DigiKey*, www.digikey.com/en/product-highlight/i/infineon/dps310-digital-barometric-pressure-sensors.

3. Industries, Adafruit. "Adafruit DPS310 Precision Barometric Pressure / Altitude Sensor." *Adafruit Industries Blog RSS*, www.adafruit.com/product/4494.

4. "Leading Manufacturer of Data Loggers for Wind and Solar Measurement." *Kintech Engineering - Systems for Wind and Solar Measurement*, www.kintech-engineering.com/.